Increasing Magnetoplasticity in Polycrystalline Ni-Mn-Ga by Reducing Internal Constraints through Porosity

Yuttanant Boonyongmaneerat,[1,*] Markus Chmielus,[2,†] David C. Dunand,[1] and Peter Müllner[2]
[1]*Department of Materials Science and Engineering, Northwestern University, Evanston, Illinois 60208, USA*
[2]*Department of Materials Science and Engineering, Boise State University, Boise, Idaho 83725, USA*
(Received 2 October 2007; published 10 December 2007)

Foams with 55% and 76% open porosity were produced from a Ni-Mn-Ga magnetic shape-memory alloy by replication casting. These polycrystalline martensitic foams display a fully reversible magnetic-field-induced strain of up to 0.115% without bias stress, which is about 50 times larger than nonporous, fine-grained Ni-Mn-Ga. This very large improvement is attributed to the bamboolike structure of grains in the foam struts which, due to reduced internal constraints, deform by magnetic-field-induced twinning more easily than equiaxed grains in nonporous Ni-Mn-Ga.

DOI: 10.1103/PhysRevLett.99.247201 PACS numbers: 75.30.Kz, 61.72.Mm, 75.80.+q

Magnetic shape-memory alloys are active materials enabling rapid, large-strain actuation upon application of a magnetic field [1,2]. The magnetic-field-induced strain is due to twin boundaries moving under the influence of an internal stress produced by magnetic anisotropy energy, and is not recovered upon removal of the field [1,3]. As such, this strain is a true plastic strain, similar to that produced by twin boundary motion induced by an externally applied stress in nonmagnetic shape-memory alloys such as Nitinol, but unlike the strain produced by lattice expansion in other magnetostrictive materials such as Terfenol D. Magnetoplasticity has been extensively studied for off-stoichiometric Ni_2MnGa Heusler alloys (e.g., [1–8]), which as single crystals exhibit large magnetoplastic strains (up to 10% when optimally oriented to the magnetic field [4,8]) due to deformation by twinning and a large magnetic anisotropy constant [2]. However, growth of Ni-Mn-Ga single crystals is slow and leads to severe segregation [9], affecting local composition, crystal structure, and magnetoplastic strain [10]. While segregation can be avoided through fast, nondirectional solidification from the melt (e.g., through melt-spinning), the resulting polycrystalline magnetic shape-memory alloys exhibit magnetoplastic strains (produced solely by magnetic forces at constant temperature and without mechanical bias stress) negligibly small as compared to single-crystal values [11]. In fact, to the authors' knowledge, no value of magnetoplastic strain has been reported in the literature for bulk, fine-grained Ni-Mn-Ga. The closest analogue is a fine-grained, melt-spun Ni-Mn-Ga ribbon (grain size of as-spun ribbons is typically 2 μm, i.e., smaller than the ribbon thickness of 20 μm [12]) displaying a very small magnetoelastic strain of 0.002% [11]. While larger strains have been found during a temperature-induced phase transformation (i.e., for the well-known shape-memory effect [13]), and with the application of a mechanical bias stress [14], the drastic decrease in magnetoplasticity for polycrystalline Ni-Mn-Ga, as compared to single crystals, can be explained by incompatibilities during twinning of neighboring grains leading to internal geometrical constraints, or, equivalently, by grain boundaries suppressing the motion of twinning dislocations [8]. Thus, reduction of internal constraints (or grain boundaries) should increase magnetoplasticity in polycrystalline Ni-Mn-Ga. Indeed, after annealing at high temperature of Ni-Mn-Ga ribbons—which leads to severe grain growth [15] with grains expected to span the ribbon thickness—the magnetoplastic strain increases by an order of magnitude, up to ~0.025% [16]. Similarly, coarse-grained materials consisting of a small number of grains show larger magnetoplasticity (e.g., 0.09% for Ni-Mn-Ga [15] and 0.013% for Co-Ni-Al alloy [17]). Here, we explore, as a strategy to improve magnetoplasticity in fine-grained polycrystalline Ni-Mn-Ga, the introduction of pores, which reduce internal constraints during twinning of neighboring grains, and whose internal surfaces do not impede the motion of twinning dislocations, unlike grain boundaries.

Open-cell Ni-Mn-Ga foams were created by the casting replication method, which has been predominantly used for low-melting Al-based foams with NaCl as space holders [18], and recently extended to a Zr-based amorphous alloy ($T_m = 842\,^\circ$C) using high-melting BaF_2 space holders [19]. This method, which results in foams with fully-dense struts and well-defined pore architecture, is extended here to an off-stoichiometric Ni_2MnGa alloy with $Ni_{50.6}Mn_{28}Ga_{21.4}$ as exact composition (with solidus and liquidus temperatures of ~1110 and ~1130 °C [9]). Sodium aluminate ($NaAlO_2$) was selected as space-holder, because of its good thermodynamic stability, high-melting point ($T_m = 1650\,^\circ$C) and ease of dissolution in acids. $NaAlO_2$ preforms were created by sintering 355–500 μm powders from Alfa Aesar (Ward Hill, MA) for 3 h in air at 1500 °C. These preforms were heated under high vacuum in an alumina crucible with inner diameter 9.5 mm to 1200 °C, infiltrated by a Ni-Mn-Ga melt under a 800 mbar pressure of 99.999% pure argon and furnace cooled. The mass difference between the metal-ceramic composite after casting and the separate phases before

casting was less than 0.4%, indicating that the average alloy composition was maintained very close to its original value. Two disks (*A* and *B*) with 3 mm thickness were cut from the infiltrated composites, from which the $NaAlO_2$ space-holder phase was leached out in an ultrasonically-agitated 10% HCl solution for 17 and 41 h, respectively. The porosity of the resulting Ni-Mn-Ga foams, as determined by helium pycnometry and Archimedes density measurements was 55% and 76%, for foams *A* and *B*. In foam *A*, space-holder removal was not complete, leaving 9 vol. % of $NaAlO_2$ in the form of undissolved powders nearly fully surrounded by metal.

Two parallelepiped samples, with approximate size $6 \times 3 \times 2.5$ mm^3, were cut from each disk and their faces were polished. These samples were homogenized (1000 °C/1 h) and then subjected to a stepwise heat-treatment for $L2_1$ chemical ordering (725 °C/2 h, 700 °C/10 h, 500 °C/20 h). One sample from each disk was additionally heated to 150 °C and furnace-cooled under a constant magnetic field of 0.5 T applied parallel to its longest edge. A similar treatment with a magnetic field parallel to the ⟨100⟩ direction is known to enhance magnetoplasticity in dense Ni-Mn-Ga single crystals [1]. These field-cooled samples are designated A_F and B_F. DSC experiments and optical microscopy indicate that the crystals are fully martensitic at room temperature. Magnetomechanical experiments were performed using a test setup described in Ref. [8], with a magnetic field of 0.97 T rotating along an axis perpendicular to the field direction at a rotation velocity of 12 000 rpm. The sample is positioned with its shortest edge parallel to the rotation axis and it is not subjected to any mechanical bias stress. The sample length was measured using laser-optical extensometers as described in more detail in Ref. [8]. Strain was recorded as a function of field direction for up to 2.5×10^7 magnetomechanical cycles.

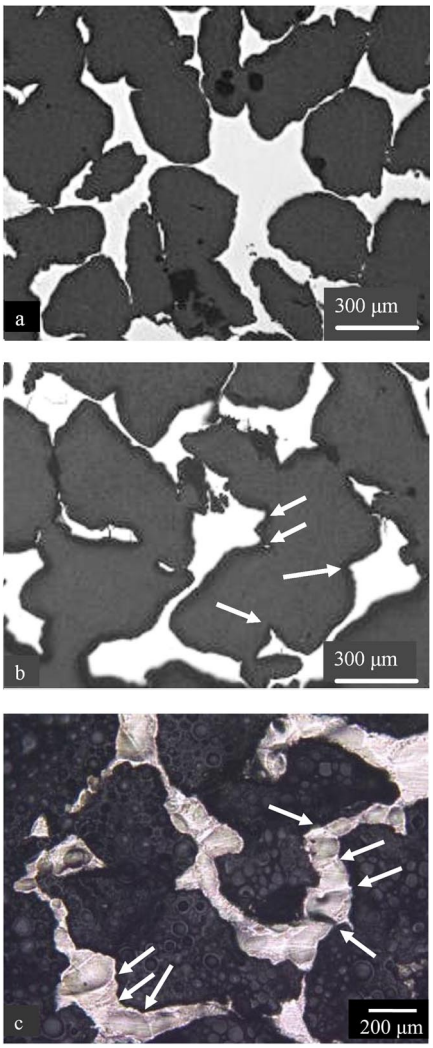

FIG. 1 (color online). Polished cross-sections (a) Foam *A* with 55% porosity, showing most struts intact and pores of similar size as the space-holder grains; (b) Foam *B* with 76% porosity, showing some dissolved struts (arrows) and pores larger than the space-holder grains; (c) Foam *B* after etching, with arrows showing prior austenite grain boundaries perpendicular to struts, corresponding to a bamboo structure.

Figure 1 shows polished cross-sections for foams *A* and *B*, confirming a lack of chemical reaction between the metal and the $NaAlO_2$ space holder. The architecture, which is typical of replicated foams, can be described by nodes connecting a network of thinner struts. Specimen *B*, which has a higher porosity due to a longer immersion time leading to complete space-holder removal and some metal dissolution by the acid, exhibits larger pores with thinner nodes and struts, some of which are truncated [as marked with arrows in Fig. 1(b)]. Grain boundaries of prior austenite grains [arrows in Fig. 1(c)] extend across struts, forming a bamboo structure. Neither grain-boundary triple junctions nor grain boundaries parallel to the strut axis were observed. The twin structure appears as surface relief in an atomic-force microscopy image (Fig. 2) on the polished faces of heat-treated foam *A*. Two twinning systems T1 and T2 produce two sets of regular parallel ridges and valleys (indicated with black arrows in Fig. 2). Twinning is visible on the entire surface indicating that the martensitic transformation is complete at room temperature.

During one full field rotation, the foam shrinks and expands twice, as illustrated in Fig. 3 for the first field revolution resulting in a magnetoplastic strain of 0.097%. Thus, the foam is subjected to two magnetomechanical cycles per field revolution. After 10^5 magnetomechanical cycles, foam *B* shows a magnetoplastic strain of 0.115% (Fig. 3). The evolution of the magnetoplastic strain amplitude as a function of magnetomechanical cycles is shown in Fig. 4 for the two types of foams. The strain for foam *A* was 0.003% which is close to the detection limit (0.002%) of the instrument. After field-cooling, foam A_F shows magnetoplastic strains initially as high as 0.065%, dropping in the range 0.010%–0.020% after about 40 cycles. Foam *B*, with higher porosity and no residual space-holder, showed even higher magnetoplastic strain values: from an initial value of 0.097%, it increased to 0.110% where it

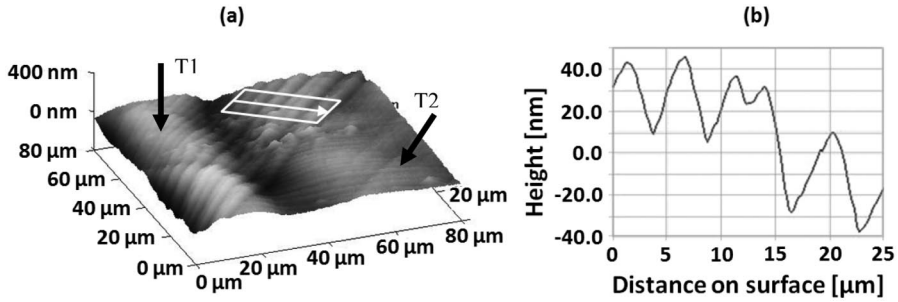

FIG. 2. Twin structure in a strut of foam A recorded with an atomic-force microscope. (a) The height-image reveals two twin variants T1 and T2 as indicated with black arrows. (b) Surface profile corresponding to the box in (a) indicates a twin thickness of approximately 2 μm.

stabilizes for nearly 1000 magnetomechanical cycles and varied thereafter in the range between 0.080% and 0.115%. After field-cooling, foam B_F exhibits somewhat reduced magnetoplastic strains of about 0.040% up to 40 magnetomechanical cycles, decreasing gradually to about 0.030% at 500 000 magnetomechanical cycles. The variation in magnetoplastic strains between these four samples is difficult to rationalize, and may be predominantly controlled by small differences in composition resulting from segregation during the nondirectional furnace cooling. Independently of these variations, the most relevant result apparent from Fig. 4 is that initial magnetoplastic strains of foams A_F, B, and B_F (0.04%–0.10%) are 20 to 50 times higher than the magnetoelastic strain (0.002%) reported for fine-grained Ni-Mn-Ga thin ribbons [11]), and 2 to 4 times higher than the magnetoplastic strain ($\sim$ 0.025% [16]) for coarse-grained Ni-Mn-Ga ribbons. The foam strains remain, however, much lower than for Ni-Mn-Ga single-crystals (up to 10% [4,8]). The trend of magnetoplastic strain decreasing from single-crystal to polycrystalline foam, to coarse-grained polycrystalline ribbon, to fine-grained polycrystalline ribbon can be qualitatively explained by an increase in constraints between neighboring grains undergoing twinning deformation, as discussed below.

In experiments with single crystals, one side of the sample is rigidly glued to an immovable sample holder. The opposite side of the sample is glued to a sled which can freely translate in one direction, imposing minimal constraints on an optimally oriented crystal [8]. In the bamboo-structured struts of the foams, individual grains are also rigidly bound to two neighboring grains, which are, however, restricted in translation (unlike a sled), because struts are connected to each other by nodes in a three-dimensional reticulated structure which constrains their displacement. The constraints, while not as severe as for a pore-free polycrystal, are much higher than for a nearly constraint-free single crystal. If the bamboo-structured struts were unconnected to each other (as in a three-dimensional aggregate, or mat, of short fibers), constraints would be further reduced and higher magnetoplastic strains would result. The fine-grained ribbons [11] have grains which are constrained in all three dimensions. Columnar grains in coarse-grained ribbons [20] span the width of the ribbon and are thus constrained only in two dimensions. This explains the improvement in magnetoplasticity as compared to fine-grained ribbons. In foams, bamboo-shape grains in struts are constrained in only one dimension leading to further improvement of magnetoplasticity. Finally, single crystals are unconstrained and thus display the maximum-achievable magnetoplastic strain as dictated by crystallography [4,8].

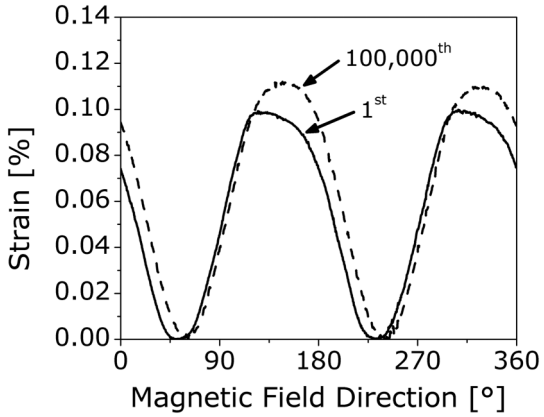

FIG. 3. Magnetic-field induced (magnetoplastic) strain for foam B for first cycle (solid line), and after 100 000 cycles (dashed line).

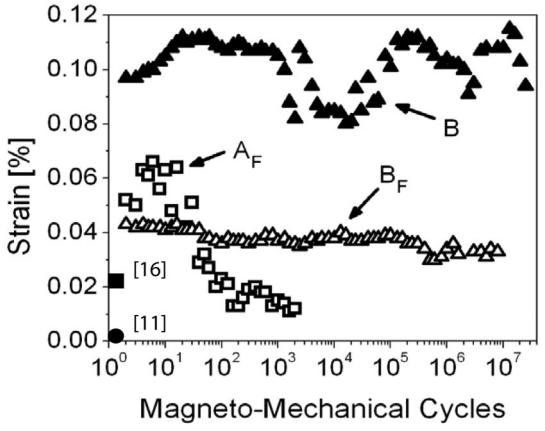

FIG. 4. Magnetic-field induced (magnetoplastic) strain as a function of the number of magnetomechanical cycles for foam A_F (55% porosity) and B, B_F (76% porosity). For comparison, the strains measured in a unidirectional (i.e., nonrotating) field for fine-grained (solid circle, [11]) and coarse-grained (solid square, [16]) ribbons are indicated.

A further illustration may be given by a thought experiment, where open porosity is created (by micromachining, chemical dissolution, or other means) in a single crystal: the magnetoplastic strain of this monocrystalline foam remains unchanged. If, however, a polycrystal is made into a foam by removal of a subset of its grains (which become porosity), the network of remaining solid still exhibits constraints when subjected to a magnetic field, and thus shows a much reduced magnetoplasticity. The present polycrystalline foams resemble the latter polycrystalline construct, and thus have magnetoplastic strains closer to those of a dense polycrystal than to a single crystal. A more complete analysis of the effect would necessitate the use of a complex finite-element model with detailed knowledge of the crystallographic orientation of grains in the struts, which is beyond the scope of the present Letter.

The 50-fold improvement shown by foam *B* as compared to the best fine-grained (i.e., bulklike) Ni-Mn-Ga thin ribbons demonstrates that nonoptimized Ni-Mn-Ga foams are comparable, in terms of strain and response time, to some of the best nonmagnetoplastic magnetostrictive materials such as Terfenol D exhibiting 0.1%–0.2% strain [21]. However, Terfenol D has a higher density and contains more expensive metals (Tb and Dy) than Ni-Mn-Ga [22], and it requires a bias stress to access its full strain potential [21], unlike for the present foams. Also, Fig. 4 shows that the magnetoplastic strain deteriorates little, for two of the four foams studied, up to the highest number of magnetomechanical cycles tested (2.5×10^7), confirming that these foams can be competitive with Terfenol D in terms of durability. Finally, it is possible to make use of the open porosity of magnetic shape-memory foams beyond the initial goal of decreasing internal constraints and boosting magnetoplastic strains, and the associated decrease in apparent density. For example, these foams could be designed to displace fluids within their pores without moving parts, or may be infiltrated with another solid, such as an elastomer, to create a composite. Alternatively, the large specific area of the foam structure may allow for magnetocaloric Ni-Mn-Ga foams with enhanced heat-transfer rates useful for magnetic refrigeration near ambient temperature [23].

In summary, we have demonstrated that porous polycrystalline Ni-Mn-Ga, with a cellular microstructure consisting of nodes and struts with bamboo-structured grains, displays a fully-reversible magnetoplastic strain as high as 0.115% with good stability over 25 million magnetomechanical cycles. This strain is at least 50 times higher than for the magnetoelastic nonporous, fine-grained polycrystalline magnetic shape-memory alloy and comparable to some of the best nonmagnetoplastic magnetostrictive materials such as Terfenol D. The magnetoplastic strain enhancement displayed by the foams is assigned to a decrease in internal constraints produced during twinning deformation in struts with bamboo grain structure. It is likely that control of the solidification procedure (to reduce segregation and to produce large textured grains) and judicious optimization of the strut architecture (to minimize internal constraints during twinning) and of thermo-magneto-mechanical training will lead to foams with further gains in magnetoplastic strains.

The authors thank Professor Gernot Kostorz (ETH Zürich) for providing the alloy ingot and Brandon Christoffersen (Boise State U.) for carrying out DSC experiments. P. M. is grateful for support by the National Science Foundation (NSF) under Grant No. DMR-0502551.

*Present address: Metallurgy and Materials Science Research Institute, Chulalongkorn University, Pathumwan, Bangkok 10330, Thailand.

†Also at Hahn-Meitner-Institut, Smart Magnetic Materials Group, SF1, 14109, Berlin, Germany.

[1] S. J. Murray, M. Marioni, S. M. Allen, R. C. O'Handley, and T. A. Lograsso, Appl. Phys. Lett. **77**, 886 (2000).
[2] K. Ullakko, J. K. Huang, C. Kantner, R. C. O'Handley, and V. V. Kokorin, Appl. Phys. Lett. **69**, 1966 (1996).
[3] P. Müllner, V. A. Chernenko, M. Wollgarten, and G. Kostorz, J. Appl. Phys. **92**, 6708 (2002).
[4] A. Sozinov, A. A. Likhachev, N. Lanska, and K. Ullakko, Appl. Phys. Lett. **80**, 1746 (2002).
[5] O. Söderberg, Y. Ge, A. Sozinov, S.-P. Hannula, and V. K. Lindroos, Smart Materials and Structures **14**, S223 (2005).
[6] I. Suorsa and E. Pagounis, J. Appl. Phys. **95**, 4958 (2004).
[7] H. E. Karaca, I. Karaman, B. Basaran, Y. I. Chumlyakov, and H. J. Maier, Acta Mater. **54**, 233 (2006).
[8] P. Müllner, V. A. Chernenko, and G. Kostorz, J. Appl. Phys. **95**, 1531 (2004).
[9] D. L. Schlagel, Y. L. Wu, W. Zhang, and T. A. Lograsso, J. Alloys Compd. **312**, 77 (2000).
[10] V. A. Chernenko, Scr. Mater. **40**, 523 (1999).
[11] P. Lazpita, G. Rojo, J. Gutierrez, J. M. Barandiaran, and R. C. O'Handley, Sensor Lett. **5**, 65 (2007).
[12] K. Otsuka and X. Ren, Prog. Mater. Sci. **50**, 511 (2005).
[13] Y. Ly, Y. Xin, C. B. Jiang, and H. B. Xu, Scr. Mater. **51**, 849 (2004).
[14] Z. Q. Zhao, S. X. Wu, F. S. Wang, Q. Wang, L. P. Jiang, and X. L. Wang, Rare Metals Letters **23**, 241 (2004).
[15] O. Söderberg, Y. Ge, N. Glavatska, O. Heczko, K. Ullakko, and V. K. Lindroos, J. Phys. IV (France) **11**, Pr8-287 (2001).
[16] S. Guo, Y. Zhang, B. Quan, J. Li, and X. Wang, Mater. Sci. Forum **475–479**, 2009 (2005).
[17] H. Liu, H. X. Zheng, Y. L. Huang, M. X. Xia, and J. G. Li, Scr. Mater. **53**, 29 (2005).
[18] Y. Conde, J. F. Despois, R. Goodall, A. Marmottant, L. Salvo, C. San Marchi, and A. Mortensen, Adv. Eng. Mater. **8**, 795 (2006).
[19] A. H. Brothers, R. Scheunemann, J. D. DeFouw, and D. C. Dunand, Scr. Mater. **52**, 335 (2005).
[20] C. V. Thompson, Annu. Rev. Mater. Sci. **30**, 159 (2000).
[21] K. Hathaway and A. E. Clark, MRS Bull. **18**, 34 (1993).
[22] US Geological Survey. Metal Prices in the United States through 1998, Reston, VA.
[23] X. Zhou, W. Li, H. P. Kunkel, and G. Williams, J. Phys. Condens. Matter **16**, L39 (2004).